JOURNAL OF CHEMICAL INFORMATION AND MODELING

Article

pubs.acs.org/jcim

Understanding the Structure–Function Relationship of Lysozyme Resistance in *Staphylococcus aureus* by Peptidoglycan O-Acetylation Using Molecular Docking, Dynamics, and Lysis Assay

Anju C. Pushkaran,[†,§] Namrata Nataraj,[†,§] Nisha Nair,[†] Friedrich Götz,[‡] Raja Biswas,*[,†] and C. Gopi Mohan*[,†]

[†]Amrita Centre for Nanosciences and Molecular Medicine, Amrita Institute of Medical Sciences & Research Centre, Amrita Vishwa Vidyapeetham University, Ponekkara, Kochi 682 041, Kerala State, India

[‡]Microbial Genetics, Interfaculty Institute for Microbiology and Infection Medicine Tübingen (IMIT), University of Tübingen, 72074 Tübingen, Germany

Supporting Information

ABSTRACT: Lysozyme is an important component of the host innate defense system. It cleaves the β-1,4 glycosidic bonds between *N*-acetylmuramic acid and *N*-acetylglucosamine of bacterial peptidoglycan and induce bacterial lysis. *Staphylococcus aureus* (*S. aureus*), an opportunistic commensal pathogen, is highly resistant to lysozyme, because of the O-acetylation of peptidoglycan by *O*-acetyl transferase (*oatA*). To understand the structure–function relationship of lysozyme resistance in *S. aureus* by peptidoglycan O-acetylation, we adapted an integrated approach to (i) understand the effect of lysozyme on the growth of *S. aureus* parental and the *oatA* mutant strain, (ii) study the lysozyme induced lysis of exponentially grown and stationary phase of both the *S. aureus* parental and *oatA* mutant strain, (iii) investigate the dynamic interaction mechanism between normal (de-O-acetylated) and O-acetylated peptidoglycan substrate in complex with lysozyme using molecular docking and molecular dynamics simulations, and (iv) quantify lysozyme resistance of *S. aureus* parental and the *oatA* mutant in different human biological fluids. The results indicated for the first time that the active site cleft of lysozyme binding with O-acetylated peptidoglycan in *S. aureus* was sterically hindered and the structural stability was higher for the lysozyme in complex with normal peptidoglycan. This could have conferred reduced survival of the *S. aureus oatA* mutant in different human biological fluids. Consistent with this computational analysis, the experimental data confirmed decrease in the growth, lysozyme induced lysis, and lysozyme resistance, due to peptidoglycan O-acetylation in *S. aureus*.

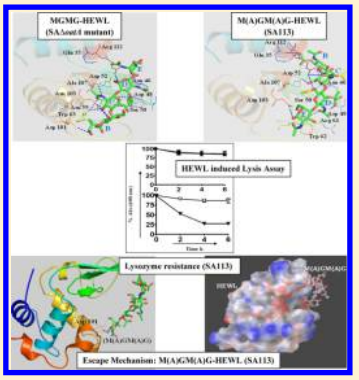

INTRODUCTION

Lysozyme, a principle component of the host innate defense system, is a 14.3 kDa cationic bacteriolytic enzyme. It is present in varying concentrations (1 μg/mL–13 mg/mL) in all human biological fluids including serum, tears, saliva, human milk and mucus. Lysozyme has two different antibacterial modes of action: (i) Lysozyme degrades peptidoglycan (PG) by catalyzing the hydrolysis of the β-1,4 glycosidic linkages between *N*-acetylmuramic acid (NAM) and *N*-acetyl glucosamine (NAG) residues in the bacterial cell walls.[1,2] (ii) Lysozyme damages bacterial membrane due to its cationic antimicrobial peptide activity.[3] *Staphylococcus aureus* (*S. aureus*), a commensal pathogen, is completely resistant to lysozyme. *S. aureus* is protected both from PG degrading and cationic antimicrobial activity of lysozyme due to its PG modification by O-acetylation and teichoic acids modification D-alanylation.[4] O-Acetylated PGs are resistant to bacteriolytic activity of lysozyme. The D-alanine esters introduce positively charged amino groups into the teichoic acid structure and prevent the cationic antimicrobial activity of lysozyme.[5,6] Although the resistance mechanism of *S. aureus* against cationic antimicrobial activity of lysozyme is well-established, but the molecular mechanism of lysozyme resistance governed by O-acetylation of NAM of PG is not yet completely known.[6]

Lysozyme has a large active binding site cleft which can accommodate tetrasaccharide to hexasaccharide subunits of the glycan chains. Subsites of lysozyme which can accommodate PG saccharides were denoted as **A**, **B**, **C**, **D**, **E**, and **F** by Imoto et al.[7] PG's binding and an enzymatic property of the lysozyme was extensively studied by different research groups. Further, it was shown that lysozyme cleaves the β-1,4 glycosidic linkage between subsites **D** and **E**. PG's productive binding and conversion to a reactive complex was only achieved with the additional binding energy provided by the interaction of either tetrameric subunits to sites **B**, **C**, **D**, and **E** or hexameric subunits to sites **A**, **B**, **C**, **D**, **E**, and **F** on lysozyme.[7−9]

A majority of pathogenic bacteria are resistant to lysozyme, and the cause of this was deciphered only recently. The pioneering work of Bera et al. elucidated the crucial role of PG

Received: October 30, 2014
Published: March 16, 2015

DOI: 10.1021/ci500734k
J. Chem. Inf. Model. 2015, 55, 760–770

O-acetylation in lysozyme resistance.[6] The gene responsible for PG O-acetylation was identified as *O*-acetyl transferase in *S. aureus* (SA2354), and the deletion mutant of *O*-acetyl transferase gene (SAΔ*oatA*) was sensitive to lysozyme.[10−13] Several pathogenic and nonpathogenic bacteria belonging to genus staphylococcus were examined by Bera et al.[6,14] They found that all pathogenic Staphylococcal strains—*S. aureus*, *S. epidermidis*, *S. saprophyticus*, *S. lugdunensis*, *S. hemolyticus*, *S. warneri*, and *S. hyicus*, which are O-acetylated—are resistant to lysozyme. Whereas all nonpathogenic Staphylococci strains—*S. carnosus*, *S. xylosus*, *S. equorum*, *S. arlettae*, *S. condimenti*, and *S. piscifermentans*, which are de-O-acetylated—are sensitive to lysozyme.[6,14]

PG, the core component of the bacterial cell wall, is a polymer of glycan chains and stem peptides. The glycan chains are composed of repeated alternating units of NAM and NAG, joined by a β-1,4 linkage. NAM residues are lactyl linked with the stem peptide, which is composed of L-Ala-D-Gln-L-Lys-D-Ala-D-Ala. The neighboring stem peptides in *S. aureus* are cross-linked through penta-glycine bridges.[10−12,15] O-Acetylation of NAM of PG and lysozyme resistance later found to be true for many Gram-positive and Gram-negative bacteria such as *Enterococcus faecalis*,[16] *Bacillus subtilis*,[17] *Bacillus anthracis*,[18] *Lactococcus lactis*,[19] and *Streptococcus pneumoniae*.[11,15,20] The extent of these PG modifications in NAM residue varies from 20% to 70% in different species (or strains). Further, the degree of O-acetylation in different species are correlated with its lysozyme resistance.[15]

Although the vital role of *oatA* in lysozyme functioning has been well studied in *S. aureus* and other bacterial strains,[6,10,14] there is a limited understanding on the molecular basis of lysozyme resistance governed by *oatA*. Further, the growth pattern of the *oatA* mutant in human biological secretions (serum, saliva, and tears) has not yet been completely explored. Thus, the main objective of the present study was to perform lysozyme induced lysis assay of both *S. aureus* parental and *oatA* mutant strain, to understand the molecular level details of the lysozyme resistance in *S. aureus*. The second objective was to understand the structure−function relationships of lysozyme−substrate interaction in *S. aureus* for two systems, i.e., lysozyme in complex with de-O-acetylated and O-acetylated tetrasaccahride subunits of PG.

METHODS

Experimental Section. *Ethics Statement.* All human biological samples viz., saliva, tears, and serum, were collected from healthy volunteers. This was undertaken after taking approval from the Institutional Ethics Committee (IEC), Amrita Institute of Medical Sciences and Research Center, Kochi, India.

Growth Conditions. *S. aureus* strain SA113 (ATCC 35556)[21] and SAΔ*oatA* mutant strain[10] were cultivated in autoclaved B medium (1% tryptone, 0.5% yeast extract, 0.5% NaCl, 0.1% K_2HPO_4, 0.1% glucose; pH 7.2) at 37 °C with 160 rpm shaking. SAΔ*oatA* mutant strain was maintained in the presence of Kanamycin (30 μg/mL).[10] In order to determine the lysozyme sensitivity of SA113 and SAΔ*oatA* mutant cells, they were cultivated in the presence of 500 μg/mL concentration of HL (human lysozyme; Sigma-Aldrich L1667) or HEWL (hen egg white lysozyme; Sigma-Aldrich L6876). To measure the bacterial growth, aliquots of bacterial cultures were collected at hourly intervals. Further, it was serially diluted and plated in B-agar plates.[22] These plates were incubated at 37 °C overnight and bacterial colonies were counted.

Lysozyme Induced Lysis Assay. HL or HEWL induced lysis of SA113 and SAΔ*oatA* mutant strains were also measured after suspending the cells in PBS buffer containing lysozyme. Briefly, overnight cultures of *S. aureus* strains were pelleted down, washed twice with ice cold PBS buffer and suspended in buffers containing 250 and 500 μg/mL of lysozyme. The initial O.D. (600 nm) was adjusted to 0.5 and decrease of O.D was measured at hourly intervals for 6 h at 37 °C.[23,24]

Survival Assay in Human Biological Samples. Serum, tears, and saliva human samples were collected and sterilized by passing through 0.2 μm filter. Further, *S. aureus* cells were grown overnight culture in B-broth, pelleted down (5000*g*, 15 min.), washed twice in sterile ice cold PBS to remove the media components, and diluted to an O.D. of 0.5 (600 nm) in serum, tears, and saliva. The tubes were incubated with agitation at 37 °C for 6 h. Samples were collected at 2 h intervals and plated on B-agar plates for enumeration of surviving colonies.[25]

Computational Methods. Molecular modeling, docking, and molecular dynamics simulation studies on tetrasaccharide (MGMG) and its C_6 O-acetylated (NAM) form along with HEWL (or HL) were carried out on a Linux workstation using Schrödinger and PyMol molecular modeling packages.

Preparation of Tetrasaccharide Subunits of PG and its C_6 O-Acetylated form. The three dimensional (3D) crystal structure of HEWL in complex with trisaccharide (NAM-NAG-NAM) subunits of PG substrate was retrieved from Protein Data Bank (PDB ID: 9LYZ)[9] with a resolution of 2.5 Å. This was the first enzyme to have its 3D structure determined by X-ray crystallography. Though better resolution structures of lysozyme are available in PDB, this 9LYZ structure was preferred, since no other 3D structure of PG substrate in complex with lysozyme was experimentally solved.

Crystal structure 9LYZ has trisaccharide subunits of PG (NAM-NAG-NAM) bound to the sites labeled as **B**, **C**, and **D** of HEWL.[9] We represented these sites as **B** (NAM), **C** (NAG), and **D** (NAM) for better clarity on lysozyme binding sites with corresponding saccharide subunits and denoted as the MGM-HEWL complex system. The crystal structure of HL (PDB ID: 2ZIL)[26] was also retrieved from the PDB for molecular docking studies to understand the molecular mechanism of saccharide subunit interactions at its active binding site cleft.

We used the crystal structure of HEWL in complex with trisaccharide subunits **B** (NAM), **C** (NAG), and **D** (NAM), in order to build the fourth subunit **E** (NAG) of the PG substrate, using ChemDraw software. We denote these tetrasaccharide subunits as MGMG. In our study, the subunits in sites **B**, **C**, and **D** are from the crystallographic coordinates of HEWL, while site **E** is from model building. Further, MGMG of PG substrate was O-acetylated at the C_6 position of NAM subunits (**B** and **D**) using ChemDraw software and denoted as M(A)GM(A)G. The chemical structure of MGMG and M(A)GM(A)G is presented in Figure S1(A,B) (Supporting Information). These structures were further prepared using LigPrep software module of Schrödinger.[27] Molecular docking studies were performed using the GLIDE (grid-based ligand docking with energetics) module of the Schrödinger software[27] for (i) MGMG substrate with the crystal structure of HEWL (and HL) and (ii) M(A)GM(A)G substrate with the crystal structure of HEWL (and HL). We denote these complex systems as MGMG-HEWL and M(A)GM(A)G-HEWL for future descriptions.

DOI: 10.1021/ci500734k
J. Chem. Inf. Model. 2015, 55, 760−770

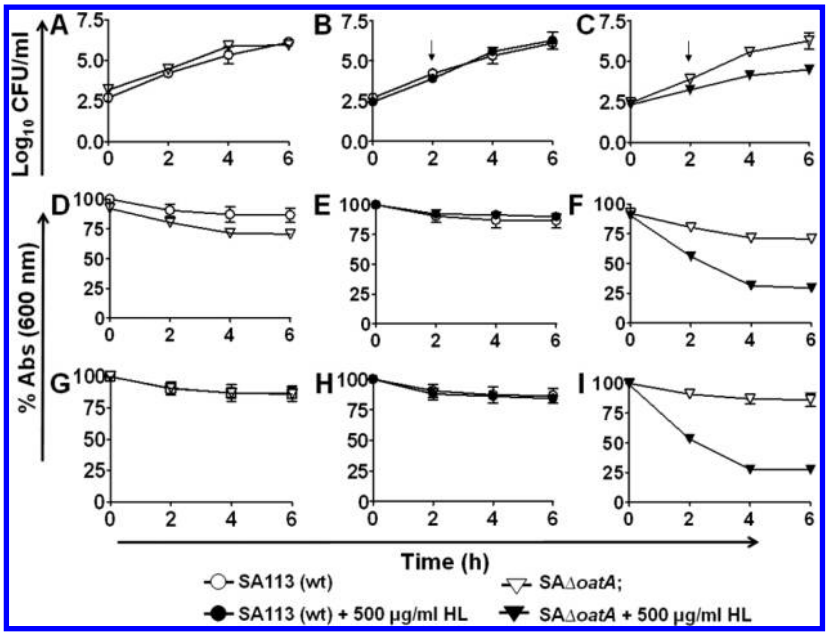

Figure 1. Growth of *S. aureus* wild type (SA113) and *S. aureus oatA* deletion mutant (SAΔ*oatA*) (**A**). Growth of SA113 in the absence or presence of 500 μg/mL HL. (**B**) Growth of SAΔ*oatA* in the absence or presence of 500 μg/mL HL (**C**). Lysozyme was added to the culture after 2 h of growth as indicated by the arrows. Lysozyme-induced lysis profile of exponentially grown (D−F) and stationary (G−I) phase cells of SA113 and SAΔ*oatA* mutant. The exponential and stationary phase cells of SAΔ*oatA* mutant were more susceptible to lysozyme induced lysis.

Molecular Docking of MGMG and M(A)GM(A)G Subunits with HEWL and HL. Crystal structure of HEWL (PDB code: 9LYZ)[9] in complex with trisaccharide subunits of PG (MGM) substrate was taken as the starting structure for our molecular docking studies using Glide program.[27] The Glide score option was selected as the fitness function in order to understand the ligand (saccharide) binding energy (BE) with respect to the target (HEWL/(or HL)) of interest. GLIDE uses a set of filters to identify the most favorable locations, i.e. pose of the ligand in the active site regions of receptor, and reports the best favorable interactions.[28] Further, the molecular grid for docking was defined using the centroid of the active site cleft residues of HEWL and HL. Scoring grids were positioned as the centroid of selected active site cleft residues of HEWL/HL (Glu35, Asn46, Asp52, Gln57, Asn59, Trp62, Trp63, Asp101, Asn103, Ala107, Trp108, and Val109) and setting these regions as the center of the grid box. Dimensions of the ligand diameter midpoint box were set equal to 14 Å (maximum). All other settings were set as default, and the option to dock flexibly with simple precision (SP) followed by extra precision (XP) was finally selected.[28]

X-ray coordinates of trisaccharide-MGM bound to the active site cleft of HEWL were used to define the active site region with an active site radius of 9.5 Å. The superimposition of the docked MGMG substrate onto crystallographic geometry of MGM yielded proper positioning of subunits MGMG at **B**, **C**, **D**, and **E** subsites of HEWL. The glide program performed well in reproducing experimentally observed binding conformation of different subunits of PG and its suitability for the present docking analysis. Finally, using the above docking protocol, MGMG and M(A)GM(A)G substrates were successfully docked at lysozyme active site cleft on both the crystal structures of HEWL and HL.

Molecular Dynamics Simulation Study of MGMG-HEWL and M(A)GM(A)G-HEWL Complex Systems. Molecular dynamics (MD) simulation study for 50 and 100 ns was performed on two systems: (i) MGMG-HEWL and (ii) M(A)GM(A)G)-HEWL using the Desmond program,[27] by keeping the temperature (300 K) and pressure (1 atm.) constant. Sodium and chloride ions were added in order to neutralize the overall charge of these two systems. Systems were solvated further using simple point charge (SPC) water model.

MD simulations were carried out with periodic boundary conditions. Prepared systems were relaxed before the simulation, which involves two steps: energy minimization and equilibration. Final equilibration was performed for both of these systems using Berendsen NPT, without any restraints on the solute. Equilibrated systems were further subjected to production simulation for 50 ns in NPT ensemble with 300 K temperature and 1 atm pressure. Energy file and trajectory coordinates were recorded at every 1.2 and 4.8 ps, respectively.

RESULTS AND DISCUSSION

Reduced Survival and Enhanced Lysis of the *oatA* Mutant in the Presence of Lysozyme. Previous work by Bera et al. demonstrated that the growth of Δ*oatA* mutant was inhibited in the presence of hen egg white lysozyme (HEWL).[6,10,14] Lysozyme was added to the culture after 2 h of growth as indicated by arrows in Figure 1B and C. We observed similar growth inhibition of Δ*oatA* mutant in the presence of human lysozyme (HL). The growth of *S. aureus* wild type (SA113) was unaltered in presence or absence of 500 μg/mL of HL (or HEWL) (Figure 1B) due to O-acetylation of NAM of its PG. The growth of SAΔ*oatA* mutant strain, which contains de-O-acetylated PG, was sensitive toward lysozyme. Addition of HL (or HEWL) into the culture of SAΔ*oatA* leads to decrease in its growth. A decrease of ∼2 log CFU/mL count was also observed after 6 h of growth compared to the control (Figure 1A and C).

Further, we measured the autolysis and lysozyme induced lysis of SA113 and SAΔ*oatA* mutant. Both exponential (Figure

DOI: 10.1021/ci500734k
J. Chem. Inf. Model. 2015, 55, 760−770

1D−F) and stationary (Figure 1G−I) phase of SA113 and SAΔ*oatA* mutant cells exhibited similar autolytic profile in PBS. The lysis of exponential (Figure 1D) and stationary phase (Figure 1G) of SA113 (wild type) and SAΔ*oatA* mutant cells were less than 20% after 6 h in the absence of HL (or HEWL). Further, lysozyme failed to induce any enhanced lysis on both the exponential (Figure 1E) and stationary (Figure 1H) phases of SA113 cells and was only 20−25% after 6 h (Figure 1E and H). When HL (or HEWL) was added, enhanced lysis of exponential (Figure 1F) and stationary (Figure 1I) phase cells of SAΔ*oatA* mutant was observed. Addition of 500 μg/mL concentration (or even less) of HL (or HEWL) finally caused 75% lysis of SAΔ*oatA* mutant after 6 h (Figure 1F and I). These experimental results clearly indicate the vital role of PG O-acetylation in hindering the catalytic activity of HL (or HEWL).

Lysozyme induced growth inhibition and enhanced lysis of SAΔ*oatA* mutant cells clearly indicates that the mutant is sensitive toward HL (or HEWL). Interestingly, lysozyme sensitivity could be explained by two ways: (i) O-acetylation of PG of SA113 prevents binding of lysozyme leading to its resistance. (ii) O-acetylation of PG hindered the accessibility of catalytic active site (β-1,4 linkages) of lysozyme and, therefore, protects SA113 from lysozyme mediated killing.

***OatA* Confers Resistance to Lysozyme in Human Biological Fluids.** Studying the effect of deletion of *oatA* gene leading to reduced survival of the mutant in human serum, saliva, and tears was performed. The survival of SA*oatA* mutant was significantly reduced in serum (p = 0.003) and tears (p = 0.028) and marginally reduced in saliva (p = 0.668) (Figure 2A−C). The lysozyme content in different biological fluids

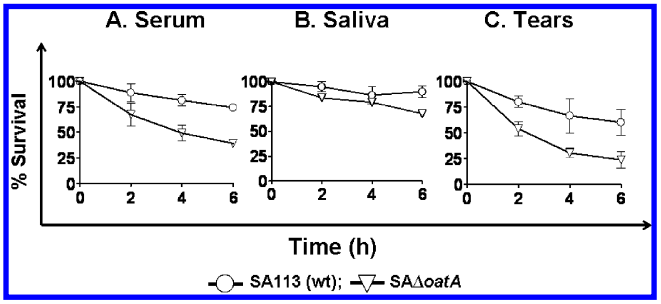

Figure 2. Survival of SA113 and SAΔ*oatA* deletion mutant in human biological fluids—serum (A), saliva (B), and tears (C). Survival of SAΔ*oatA* deletion mutant was reduced in all human biological fluids compared to wild type (SA113).

differs considerably (20 μg/mL−2 mg/mL).[29−31] These differences lead to a difference in the survival rate of SA113 and SAΔ*oatA* mutant cells, i.e., survival of SA113 and SAΔ*oatA* mutant was 74% and 39%, in serum (Figure 2A); 90% and 68% in saliva (Figure 2B); and 60% and 20% in tears (Figure 2C). Reduced survival of SAΔ*oatA* mutant in these human biological fluids indicates the vital role of OatA in *S. aureus* pathogenesis.

Structure-Based Molecular Docking of Lysozyme with Tetrasaccharide PG Subunits. A structure−function relationship of PG O-acetylation in lysozyme resistance was computationally examined. Computational techniques offer attractive alternatives to experimental methods (X-ray crystallography and NMR) for the study of protein−carbohydrate complexes. In particular, the molecular docking technique provides key information about protein−ligand interactions in systems that are difficult to study with experimental techniques.[32−35]

The crystal structure of HEWL complexed with trisaccharide PG subunits (MGM)[9] was taken as the starting structure for docking studies using Glide program.[28] It is well-known that HEWL cleaves in PG substrate at the β-(1,4) glycosidic bond linkage between NAM bound to site **D** and NAG bound to site **E** of lysozyme. Thus, a fourth subunit (NAG) was added to the existing trisaccharide subunits of PG. We selected this crystal structure because it provided more confidence in building the fourth subunit of PG substrate (namely **B** (NAM), **C** (NAG), **D** (NAM), and **E** (NAG)), by retaining the original crystal conformation (MGM) for its three (**B**, **C**, and **D**) subunits. In order to understand the interaction between lysozyme and PG with or without O-acetylation, we build two different systems: (i) tetrasaccharide subunits of PG substrate (MGMG; which mimics the PG structure of SAΔ*oatA* deletion mutant) in complex with lysozyme and (ii) C_6 O-acetylated at NAM (**B** and **D** subsites) denoted as (M(A)GM(A)G; which mimics the PG structure of SA113 wild type) in complex with lysozyme. Further, the MGMG and M(A)GM(A)G molecule was modeled in the same manner by retaining its trisaccharide (MGM) crystal conformation.

Agostino et al. performed molecular docking of carbohydrate ligands to the crystal structure of antibodies by using different molecular docking software (Glide, GOLD, FlexX, and Autodock) and revealed that Glide was the best among them.[36] We performed flexible molecular docking studies on tetrasaccharide subunits of PG (MGMG and M(A)GM(A)G) with the lysozyme using Glide software for revealing the saccharides fitting to the HEWL active binding site cleft. Figure 3A shows the superimposed projection of the de-O-acetylated trisaccharide MGM (green color) and tetrasaccharide MGMG PG subunits (pink color) with **B**, **C**, **D**, and **E** subsites of HEWL. Further, superimposition of the trisaccharide MGM (green color) and O-acetylated tetrasaccharide PG subunits M(A)GM(A)G (brown color) with **E**, **D**, **C**, and **B** subsites of HEWL is presented in Figure 3B.

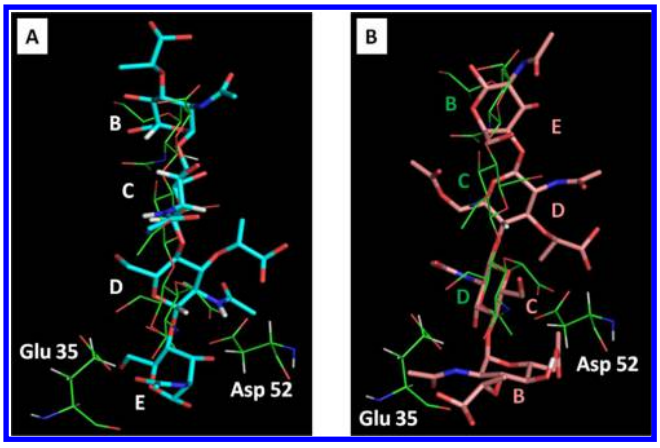

Figure 3. Superimposed projection of trisaccharide subunits (MGM-(**B**, **C**, and **D**)) of PG (green color) in the wild type with the docked conformation of tetrasaccharide subunits (MGMG-(**B**, **C**, **D**, and **E**)) of PG (pink color) in HEWL (**A**) and trisaccharide subunits (MGM-(**B**, **C**, and **D**)) of PG (green color) in wild type with the docked conformation of the O-acetylated tetrasaccharide subunits (M(A)-GM(A)G-(**E**, **D**, **C**, and **B**)) of PG (brown color) in HEWL (**B**). The positions of key catalytic cleavage site residues Glu35 and Asp52 of HEWL are also shown in stick model.

DOI: 10.1021/ci500734k
J. Chem. Inf. Model. 2015, 55, 760−770

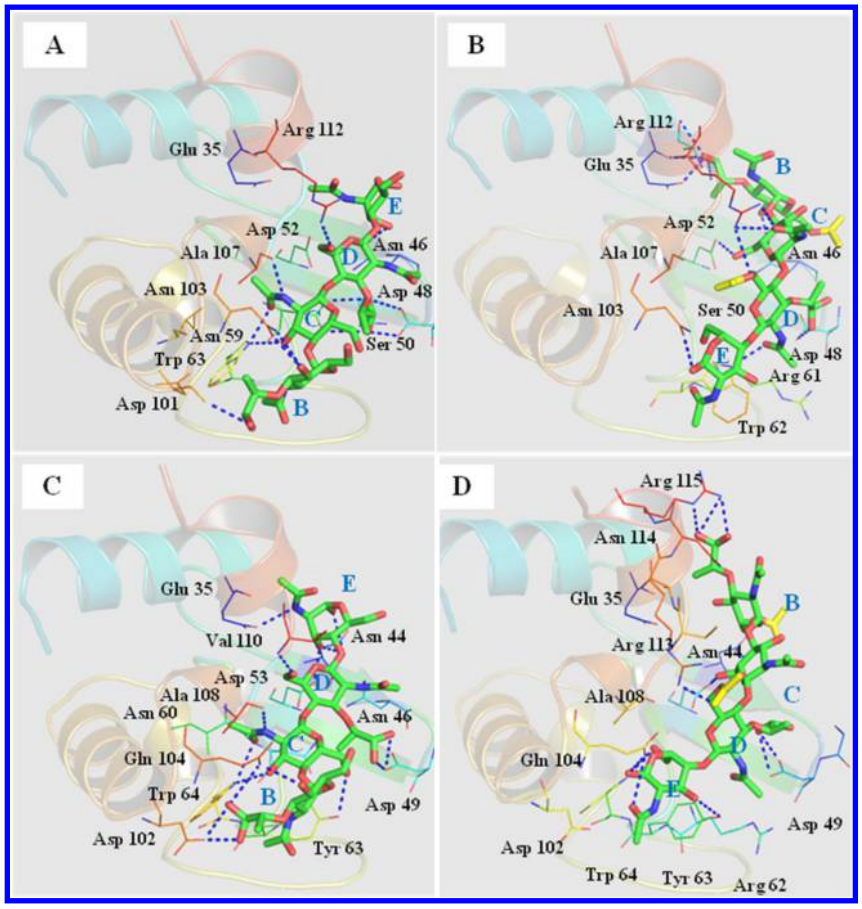

Figure 4. MGMG interacting with the active site cleft of HEWL (**A**); (M(A)GM(A)G) interacting with active site cleft of HEWL (**B**); MGMG interacting with active site cleft of HL (**C**); (M(A)GM(A)G) interacting with active site cleft of HL (**D**). Ligands are represented as thick sticks, active site residues, as thin sticks, and hydrogen bonds, as blue dashed lines. O-Acetylated regions are shown as yellow sticks in the (M(A)GM(A)G) substrate.

It is well-known that HEWL has active site architecture very similar to that of several other β-retaining glycosides, wherein two important carboxyl groups of Glu35 and Asp52 residues are separated by ∼5.0 Å away from each other. This suggests a common catalytic mechanism among these family of proteins and which is in consonance with that of HEWL/HL.[9,38] We also observed similar binding mode and distance of 5.2 Å between carboxyl groups of Glu35 and Asp52 residues in MGMG-HEWL (or HL) complexes in the present studied system (Figures 3 and 4). Thus, our docking guided predictive complex systems were accurate enough and its 3D architecture was in consonance with that of the experimentally solved crystal structure of MGM-HEWL complexes.[9]

The present study revealed for the first time the following: (i) de-O-Acetylated tetrasaccaharide (MGMG) subunits interact with the HEWL active site clefts (β-1,4 linkage between PG and the **D** and **E** sites of HEWL was directly accessible to its catalytic residues Glu 35 and Asp 52 by hydrogen bonding, and thereby forming lysis of β-1,4 linkage possible).[9] These include the first subunit "M" interaction with the **B** site of lysozyme; second subunit "G" interaction with the **C** site of lysozyme; third subunit M interaction with the **D** site of lysozyme; and the fourth subunit M interaction with the **E** site of lysozyme, respectively. This is depicted in Figure 4A. (ii) Interactions between O-acetylated tetrasaccaharide (M(A)GM-(A)G) subunits with the HEWL active site clefts were sterically hindered (β-1,4 linkage between O-acetylated PG and the **D** and **E** sites of HEWL was not directly accessible, and lies far away from its catalytic residues Glu 35 and Asp 52 by hydrogen bonding, making the lysis of β-1,4 linkage impossible). Our docking study clearly predicted this steric hindrance, and the mode of binding of M(A)GM(A)G subunits with HEWL was exactly in an opposite manner to the MGMG subunits, i.e. first subunit "M(A)" interacts with **E** site; second subunit G interacts with **D** site; third subunit M(A) interacts with **C** site; and fourth subunit G interacts with **B** site of lysozyme, and is presented in Figure 4B. Similar docking results were obtained using HL (data not shown) by taking its crystal structure. This atomic level detail analysis obtained from our molecular superimposition and docking studies revealed for the first time how O-acetylation of PG in *S. aureus* leads to lysozyme resistance.

Different catalytic mechanisms using various experimental techniques were proposed for HEWL which include: (i) Phillip's mechanism, (ii) Koshland's mechanism, and (iii) most recently, David's mechanism.[9,37,38] These mechanisms further supported the formation of Michaelis complex between saccharide subunits of PG substrate and HEWL.[9]

Further, we observed that MGMG subunits penetrates more deeply into the active site cleft of HEWL than its corresponding MGM subunits, as evident from its crystal structure.[9] We broadly obtained similar binding features when HL structure was used for docking studies with MGMG and M(A)GM(A)G subunits using Glide software.

DOI: 10.1021/ci500734k
J. Chem. Inf. Model. 2015, 55, 760−770

Table 1. MD Snapshots of HEWL-MGMG and HEWL-M(A)GM(A)G Complex Systems at 0, 10, 30, and 50 ns and Corresponding Key Residues at Different Subsites (B, C, D, and E) of HEWL Involved in Dynamic Hydrogen Bonding Interactions with Its Substrate

	HEWL-MGMG		HEWL-M(A)GM(A)G	
simulation time	hydrogen bonding interaction residues	hydrophobic interaction residues	hydrogen bonding interaction residues	hydrophobic interaction residues
0 ns	**B:** Asp101, Asn103 **C:** Trp63, Ala107 **D:** Asn46, Asn59, Asp48, Arg61,Arg112 **E:** Asn46, Asp52	Gln57, Asn44, Thr47	**B:** Glu35, Asn46, Asp52 **C:** Asp52, Arg112 **D:** Asp 48, Trp62 **E:** Asn103	Arg61, Asn106, Ala107, Val109, Gln57
10 ns	**B:** Arg61, Trp62, Arg112 **D:**Arg61, Trp62, Arg112 **E:** Asn46, Thr47, Asn59	Trp63, Asn59, Val109	**B:** Asn46 **C:** Asp48 **D:** Asn59 **E:** Asp101	Ala107, Trp63, Val109, Thr47
30 ns	**B:** Asp101 **C:** Asn46 **D:** Asp48, Asn46, Arg112 **E:** Thr47, Asn46	Arg45, Asn 59, Leu 75	**B:** Asn 46, Thr 47 **E:** Asp101	Ala107, Gly102, Trp62
50 ns	**D:** Asp48, Arg61, Arg112 **E:** Thr47	Arg45, Asn 59, Leu75, Val109	**E:** Asp101	Ala103, Ala107, Gly102, Trp62, Asp48
		Crystal Structure (HEWL-MGM)[a]		
normal state	**B:** Asn103 **C:** Trp62, Ala107 **D:**Glu35,Asn46,Val107			

[a]Crystal structure of HEWL in complex with MGM units.[9]

The binding energy (BE) computed using Glide module between HEWL and MGMG subunits for the wild type was −8.02 kcal/mol, while that between HEWL with M(A)GM(A)G in *S. aureus* was −8.93 kcal/mol respectively (Figure 4A and B). The crystal structure of MGM in complex with HEWL was available as mentioned earlier,[9] and we observed a similar mode of binding when MGM was docked with HEWL with slight increase in its BE −9.63 kcal/mol. Similar observations are obtained for HL as shown in Figure 4C and D. These computational results imply that there is no significant variation in BE of MGMG and M(A)GM(A)G subunits in the active site cleft of the HEWL (or HL), even though their binding mode varies considerably, as explained above. Our experimental results described earlier also revealed similar binding of lysozyme with SA113 and SAΔ*oatA* mutant, respectively.

It is well-known that enzymatic catalytic mechanisms were very difficult to study with the experimental techniques. Alternately, these computational analyses could provide significant insight on these molecular mechanisms. Our studied two complex systems, MGMG-HEWL (or HL) and M(A)GM(A)G-HEWL (or HL), made different types of interactions such as hydrogen bonding, van der Waals, and hydrophobic at the active site cleft residues of lysozyme with significant BE and are presented in Figure 4.

Interacting residues shown in Figure 4 do play a critical role in understanding the normal lysozyme catalytic mechanisms and its distortion in *S. aureus* due to O-acetylation. In other words, this structure−function relationship study in turn clearly illustrates the two fundamental catalytic reaction mechanisms: (i) de-O-acetylated PG substrate binding mechanism with the HEWL/(HL) by causing the lysis of the β-1,4 glycosidic linkage and (ii) O-acetylated form of NAM in PG substrate (*S. aureus*) binding mechanism with HEWL/(HL) showing hindrance for the lysis of β-1,4 glycosidic linkage in this microorganism. Experimental study on autolysis and lysozyme induced lysis described earlier also supports the above predicted mechanisms. SA113 wild type showed no enhanced lysis on addition of HEWL (or HL) in comparison to that of SAΔ*oatA* mutant cells in which 75% lysis observed (Figure 1).

Molecular Dynamics Simulation Study of MGMG-HEWL/HL and M(A)GM(A)G-HEWL/HL Complex Systems. The molecular dynamics (MD) simulation technique plays a major role in deciphering the dynamic structure−function relationships of biomolecular systems. MD simulations have been extensively applied for the refinement of structures derived from X-ray diffraction and NMR data. This technique is also used for understanding the dynamic mechanism of an enzyme and its inhibitory action.[39−43]

MD simulation study is crucial in understanding the HEWL (or HL) catalytic mechanism (substrate binding and product release), structural stability, and the dynamic fluctuations in its conformations. Such complex molecular mechanisms are not readily accessible by most of the experimental techniques for determining structure or dynamic properties between protein−substrate complexes. We performed 50 ns MD simulation for (i) MGMG-HEWL (or HL) and (ii) M(A)GM(A)G- HEWL (or HL) complex systems using DESMOND software.

Investigation of the dynamic hydrogen bonding interactions between these two complex systems during 50 ns MD simulations revealed several new significant observations including its atomic level dynamic molecular motions. Several dynamic variations of the hydrogen bonds (different hydrogen bond breaking and making) as well as other weak interactions during 50 ns time interval were explored. This will further provide an insight on the molecular mechanism of action of these two complex systems. Earlier, static models obtained by molecular docking technique do not provide sufficient insight on these dynamic changes in substrate conformations.

Interestingly, we took MD simulation trajectory snapshots of these two complex systems at four different time intervals i.e. 0,

DOI: 10.1021/ci500734k
J. Chem. Inf. Model. 2015, 55, 760−770

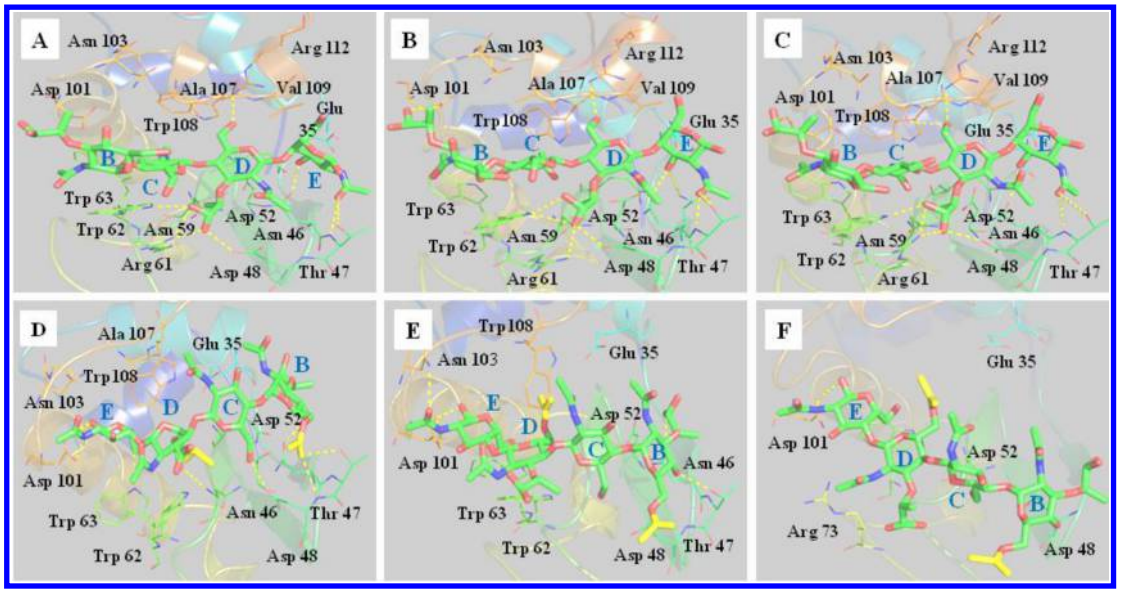

Figure 5. Snapshots of the dynamic mode of binding of HEWL-MGMG at 10 (A), 30 (B), and 50 ns (C) and HEWL-M(A)GM(A)G at 10 (D), 30 (E) and 50 ns (F) during 50 ns of MD simulation. Ligands are represented as thick sticks, active site residues, as thin sticks, and hydrogen bonds, as yellow dashed lines. O-Acetylated regions are shown as yellow sticks in the M(A)GM(A)G substrate.

10, 30, and 50 ns. Key residues involved in the mode of action at different dynamic subsites (**B**, **C**, **D**, and **E**) of HEWL are presented in Table 1 and Figure 5. Key observations in dynamic MGMG-HEWL complexes include the following: (i) Hydrogen bonds dynamically vary from 4 to 11 in this complex system. (ii) Asp48 and Arg112 hydrogen bonding interactions were stable and continuous throughout 50 ns of MD simulation. (iii) Thr47 hydrogen bonding was also stable after 10 ns of MD simulation. (iv) Arg61 hydrogen bonding showed fluctuations during MD simulation and occurs until 10 ns and breaks by 30 ns, further reforming in the 50 ns time interval. (v) Other residues hydrogen bond forming and breaking were also shown for this complex system at different **B**, **C**, **D**, and **E** subsites in HEWL. (vi) Key HEWL cleavage residues Glu35 and Asp52 are shown to be properly positioned to interact with MGMG subunits of PG substrate. (vii) Fundamental lysozyme cleavage mechanisms can be understood broadly by this dynamic complex system (MGMG-HEWL) (Figure 5A–C). In the M(A)GM(A)G-HEWL complex system the following key dynamic observations were made: (i) Hydrogen bonds dynamically vary from 1 to 8 in this complex system. (ii) The binding mode of tetrasaccharide subunits M(A)GM(A)G was reversed in the present case to subsites **E**, **D**, **C**, and **B** of HEWL, thereby differing in its lysozyme binding site residues (Figure 5D). (iii) Initially, different subunits M(A)GM(A)G of PG (in *S. aureus*) made strong interactions at (**B**, **C**, **D**, and **E**) subsites with HEWL (0–10 ns), but after 30 ns, it showed a tendency to break most of the strong and weak interactions with HEWL, thereby adopting an escape mechanism. (iv) Asp101 residue only made continuous interactions with M(A)GM(A)G subunits at the **E** subsite (HEWL) during 50 ns MD simulations. Thus, in *S. aureus* (SA113), the above-mentioned series of complicated dynamic molecular phenomenon occurred in which substrate [M(A)GM(A)G] undergone substantial strain energy effect by adopting an escape mechanisms (Figure 5E and F). Further, different weak interactions such as hydrophobic and van der Waals played an important role in these two complex systems, thereby explaining its fundamental molecular mechanism of actions.

The importance of MD simulation study thus revealed the stability of the complex formation of these two systems from static phase to dynamic phase. BE as explained earlier on the static model system shown almost equal preference to both MGMG and M(A)GM(A)G toward lysozyme. Further, MGMG-HEWL was highly stable throughout 50 ns MD simulations, as expected, for undergoing normal lysozyme catalytic reaction mechanisms. But, we encountered high instability for M(A)GM(A)G-HEWL complex system during MD simulations, even though its BE showed similar trend to that of MGMG-HEWL complexes. Further, M(A)GM(A)G do not occupy proper position in lysozyme active site cleft as explained earlier obtained using Glide software. Static and dynamic form of second complex system was interesting. It showed the tendency of binding strongly at the static phase initially, and which further undergone an "escape mechanism" in the dynamic phase revealing its weaker affinity (steric hindrance). Clarke et al. also reported similar observations in lysozyme-MurNAc complex systems showing weaker affinity due to steric hindrance of the PG substrate towards lysozyme.[43]

The importance of water molecules near the cleavage site of lysozyme was also taken into consideration in our computational studies. Conserved water molecules observed in four different crystal structures of HEWL and HL were identified in which crystal structure of HEWL, i.e. 9LYZ showed single water molecule (W188) conservation, which is nearer to the cleavage site (**D** and **E** subsites of HEWL in complex with MGMG PG substrate). W188 had a hydrogen bonding distance of 2.4 Å with Oδ2 atom of Asp52 and with the N_2 atom of NAM (**E** subsite) of MGMG making 2.5 Å. Water molecules therefore played a key role in lysozyme catalytic mechanisms. For HL, the crystal structure 2ZIL showed W241 water molecule as conserved near the cleavage site, and it made week hydrogen bonding distance of 3.0 Å with Oδ2 atom of Asp53, and which is very close to the **E** subsite of MGMG.

Studying the dynamic mode of binding of tetrasaccharide subunits of PG substrate to HEWL/HL during 50 ns of MD simulation revealed that, as expected, the structural stability and binding of MGMG is more toward HEWL (and HL), in

DOI: 10.1021/ci500734k
J. Chem. Inf. Model. 2015, 55, 760–770

comparison to that of M(A)GM(A)G acetylated form present in *S. aureus* (Figure 5). Interestingly, it was observed that after 20 ns of MD simulation, M(A)GM(A)G showed a tendency to move away from the active site cleft of HEWL/HL (Figure 5E). After 45 ns, M(A)GM(A)G partially escaped from the active site cleft of (**B**, **C**, and **D**) subunits in HEWL (or HL) and the Asp101 residue in the **E** subunit is only making a single hydrogen bond with its substrate, as shown in Figure 5F. Phillips et al. also performed MD simulations of HEWL alone and with a bound substrate (hexa-*N*-acetyl glucosamine) to understand the structure and dynamics of protein.[44]

In order to check the consistency of the above-mentioned MD results for 50 ns, we repeated the simulation for the 100 ns time interval in both the systems (i) HEWL-MGMG and (ii) HEWL-M(A)GM(A)G. The increase in the MD simulation time from 50 to 100 ns will significantly provide better insight and confidence to our predicted results by understanding the dynamic structure−function relationships for MGMG normal interaction and M(A)GM(A)G escape mechanisms toward the active site cleft of lysozyme.

Interestingly, the MD simulation results for 50 and 100 ns of these two complex systems are broadly similar, except for a few minor variations we observed during the dynamic interaction between HEWL with M(A)GM(A)G. Further, we observed consistency in the MD results of the first system (HEWL-MGMG), and the complex was structurally stable throughout 100 ns simulations, as expected.

For the second complex system (HEWL-M(A)GM(A)G) during the 100 ns MD time interval, we observed structural instability in the system, in which M(A)GM(A)G adopted an escape mechanism toward lysozyme. A similar type of observation was seen in the 50 ns MD simulations described earlier. We further observed some minor changes in the interacting residues within the subsites of lysozyme on binding toward M(A)GM(A)G for 50 and 100 ns MD simulations. But, the trend of variation in the dynamic interactions observed by M(A)GM(A)G for its escape mechanisms from the lysozyme active site cleft remains broadly the same, irrespective of its 50 or 100 ns MD simulation time. Further, we noted following minor changes by increasing the MD simulation time from 50 to 100 ns: (i) Asp101 residue made hydrogen bonding interaction with the M(A)GM(A)G at 50 ns (last frame), and this was modified to Gly102 residue, by analyzing the 50 ns frame of 100 ns MD simulations. But, both of these residues belong to the **E** subunit in lysozyme. (ii) At the 50th ns frame, the Asp101 residue made a hydrogen bonding interaction with M(A)GM(A)G as mentioned earlier (Table 1), but it was changed to the Ser24 residue in the 100th ns frame (last frame). Interestingly, both of these residues (Asp101 and Ser24) are very far away (~25.0 Å) from the active site cleft regions of lysozyme. This in turn suggests lysozyme inability to function normally in *S. aureus* (SA113), thereby causing resistance due to O_6-acetylated M(A)GM(A)G substrate.

Further, during MD simulations we observed a dynamic variation in molecular electrostatic potential (EP) surfaces of M(A)GM(A)G binding at the active site cleft of HEWL, showing its escape mechanism (Figure 6A and B). All the above-mentioned molecular docking guided dynamics simulation studies thus confirms high steric strain (or conformational changes) observed by O_6-acetylated [M(A)GM(A)G] substrate on binding to the active site cleft of lysozyme in *S. aureus* (or SA133).

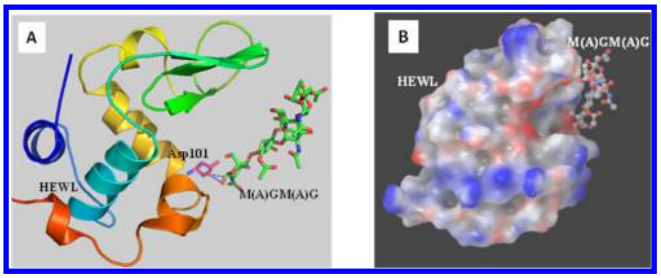

Figure 6. Dynamic mode of binding between the (M(A)GM(A)G)-HEWL complex structure obtained at 50 ns of MD simulation and showing an escape mechanism of substrate from lysozyme active site cleft. M(A)GM(A)G is shown as a stick model, and HEWL as a cartoon model (**A**). Electrostatic potential surface map of HEWL with M(A)GM(A)G in ball and stick model showing the displacement of tetrasaccharide PG substrate (**B**). EP scales are color coded with maximum positive potential (+10 kcal/mol) in red and maximum negative potential (−10 kcal/mol) in blue.

Molecular Mechanisms of Lysozyme Resistance in *S. aureus*. Molecular docking guided dynamics simulations study revealed for the first time the major conformational changes observed due to O_6-acetylation of PG substrate on binding to lysozyme. Docking of MGMG and M(A)GM(A)G substrate toward the active site of lysozyme using Glide[28] program showed differences in the static mode of binding between these complex systems (Figure 3 and 4).

An understanding of both the complex structural rearrangements and changes in the conformational properties induced by the deacetylated and acetylated PG substrate binding is therefore important for the analysis of lysozyme enzymatic reactions. Catalytic mechanism of lysozyme and its family member β-glycosides occurs by the formation and subsequent breakdown of the PG covalent intermediate species, which in turn was supported by different experimental techniques, including mass spectrometry and kinetic isotope effects.[38] These mechanisms were in consonance with the C_1 electronic migration along the reaction coordinate, principle of least nuclear motion, antiperiplanar lone pair hypothesis, substrate distortion proposed by Phillips and the covalent intermediate formation suggested by Koshland.[9,37]

It has been well-established by different research groups that the saccharide subunits of PG found in cell walls of bacteria recognize the lysozyme active site cleft for its catalytic reactions. Each glucopyranose ring of PG during interactions with lysozyme adopts the $^{2,3}C_1$ chair conformation (at positions **B** and **C**), except the fourth unit $^4C_1$ having half chair (or sofa) strained conformation (at position **D**).[9,37] Similar observations were predicted in our lysozyme-MGMG complexes obtained using Glide docking technique, shown in Figure 3A. Further, lysozyme cleaves the β-1,4 glycosidic linkage due to steric strain observed by the fourth saccharide unit, where the C_1 carbon of M (at position **D**) is connected to C_4 carbon of adjacent subunit G (at position **E**).

Stabilization of the transition state carbonium ion of the fourth subunit M (of PG substrate) in site **D** of lysozyme is replaced with G subunit in O-acetylated PG substrate of *S. aureus* (Figures 3 and 4). This phenomenon leads to large structural and conformational changes of M(A)GM(A)G substrate binding to lysozyme, which in turn do not support the transition state formation of M(A) subunit, as mentioned above, leading to complete stoppage of its catalytic reaction mechanisms in *S. aureus* (SA113). Further in M(A), where O_6

DOI: 10.1021/ci500734k
J. Chem. Inf. Model. 2015, 55, 760−770

gets acetylated, the lactone ring of NAM has bulky lactyl substituent, which further increases its surface area. So, the bulky saccharide unit of NAM in *S. aureus* (M(A)) causes steric hindrance on binding to the active site cleft of lysozyme leading to improper binding of bacterial PG. In other words, the position occupied at the β-1,4 glycosidic bond cleavage (or site **D** of lysozyme) was G instead of M in *S. aureus*. Further, the presence of GM(A) distorts the conformation of the M(A)-GM(A)G-lysozyme binding complexes, causing high steric strain observed in the present molecular docking guided dynamics simulation (Figure 5). Residues interacting with the C_6−OH group of NAM (4th saccharide subunit and site **D** of lysozyme) in MGMG-lysozyme were Arg112 (hydrogen bonding interaction with the O_6 atom of saccharide ring) and Val109 (hydrophobic interactions with the saccharide ring) shown in Figures 4 and 5. The corresponding region of O-acetylated NAM of PG in *S. aureus* was Thr47 and Asp48 residues (site **B** of lysozyme), making hydrophobic interactions with (M(A)) subunit of the tetrasaccharide substrate, respectively. But these residues are far away from the catalytic residues (Asp52 and Glu35) of lysozyme where cleavage is supposed to take place. Further, the catalytic residues of lysozyme at the **D** and **E** regions do not make any direct interactions with the M(A)G subunits of bacterial PG, where in the normal case cleavage takes place (Figure 5). All these complex dynamic molecular phenomena observed during 50 and 100 ns, MD simulations favor large conformational changes of O-acetylated PG substrate leading to lysozyme resistance in *S. aureus*. A flowchart of the reaction scheme adopted in the present work using molecular docking guided dynamics simulation for these complex systems is depicted in Figure 7.

Thus, by investigating the dynamical motion of both these complexes (MGMG-lysozyme and M(A)GM(A)G-lysozyme), we could be able to reveal extremely valuable indication of the atomic level details of the PG conformational changes. Furthermore, subtle dynamic differences in the PG substrate-binding subsites could be detected by MD analysis, and this in turn may contribute to the recognition of the molecular events in lysozyme-substrate interactions. MGMG−lysozyme complexes were very stable throughout (50 or 100 ns) MD simulations. But, in the case of M(A)GM(A)G-lysozyme complexes, MD simulation study showed high instability after 30 ns time interval (Figure 5). This in turn lead to large conformational changes in bacterial PG by breaking most of the hydrogen bonding and other weak interactions with lysozyme, and thereby adopting an escape mechanism (Figures 5**D**, **E**, and **F**). Thus, the present results clearly signify that the drastic internal structural variations of PG conformations at the atomic level is closely related to the lysozyme inability to function properly and thereby causing resistance in *S. aureus* (SA113).

It will be clear from the present study that although lysozyme resistance in *S. aureus* (SA113) has not been seen in action, we have succeeded in building up a detailed picture of how it may work. There is already a great deal of experimental evidence in agreement with this picture, and as the result of all the work was now in progress, we can be sure that the structure−function relationships of lysozyme resistance will soon be fully understood in pathogenic species. Our integrated study thus revealed the molecular mechanism of bacterial PG O-acetylation contribution toward lysozyme resistance.

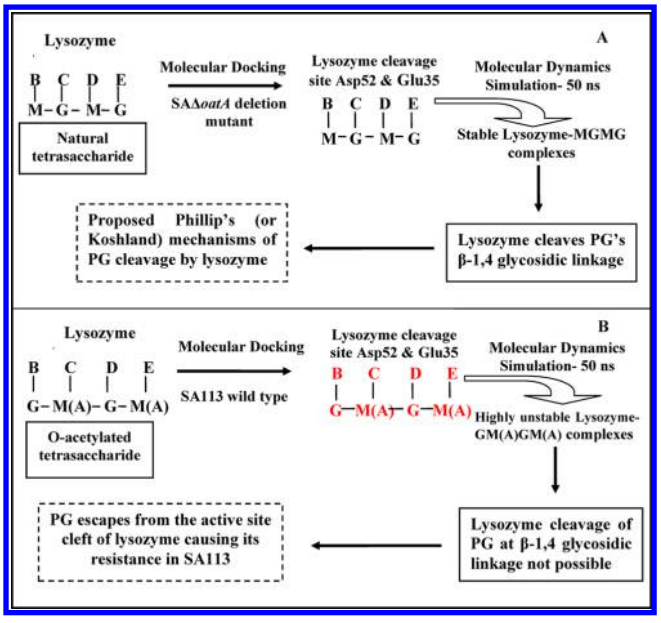

Figure 7. Flowchart showing the conformational mechanisms observed in HEWL-MGMG and HEWL-M(A)GM(A)G complex systems depicting the normal lysozyme function (A) and its resistance in *S. aureus* (SA113) (B).

SUMMARY AND CONCLUSIONS

This is the first report where molecular mechanism of lysozyme resistance in *S. aureus* by PG modifications was addressed by integrating biochemical and computational techniques. PG modification in pathogens is a common mechanism to prevent degradation and bacterial lysis on exposure to host antimicrobials leading to increased inflammation at the site of infection. Lysozyme induced lysis assay on SA113 parental showed resistance while SAΔ*oatA* mutant strain do not showed any resistance, as expected. Similar observations were obtained in the computational study using molecular docking followed by MD simulations (50 or 100 ns) in MGMG-lysozyme and M(A)GM(A)G-lysozyme complex systems. MGMG-lysozyme system, as expected, occupied proper position in the active binding site cleft of lysozyme in order to undergo its normal catalytic mechanism, and the complex was also highly stable during MD simulations. But, the second system (M(A)GM-(A)G-lysozyme) was highly distorted and the saccharides occupied different positions with higher instability during MD simulations. Further, M(A)GM(A)G had undergone an escape mechanism, due to its high strain energy or steric interference leading to lysozyme resistance in *S. aureus*. Thus, by integrating experimental and computational techniques we obtained structure−function relationships of bacterial PG O-acetylation involvement in the lysozyme resistance in *S. aureus*.

ASSOCIATED CONTENT

Supporting Information

Figure S1: Tetrasaccharide subunits of natural substrate PG (NAM-NAG-NAM-NAG) (or MGMG) with the cleavage site shown by dotted red lines (A). Tetrasaccharide subunits of PG (NAM-NAG-NAM-NAG) (or M(A)GM(A)G) substrate with NAM (**B** and **D**) O-acetylated at C_6 position (B). The acetylated moiety is shown in a red circle for clarity. This material is available free of charge via the Internet at http://pubs.acs.org.

DOI: 10.1021/ci500734k
J. Chem. Inf. Model. 2015, 55, 760−770

AUTHOR INFORMATION

Corresponding Authors

*E-mail: cgmohan@aims.amrita.edu. Tel.: +91 0484 4001234 (Extn 8769). Fax: +91 0484 2802020 (C.G.M.).

*E-mail: rajabiswas@aims.amrita.edu. Tel.: +91 0484 4001234 (Extn 8764) (R.B.).

Author Contributions

§A.C.P. and N.N. contributed equally to this work. R.B. and C.G.M. designed the experiments. A.C.P., N.N., and N.N. performed the experiments. C.G.M., R.B., and F.G. analyzed the data and wrote the paper.

Notes

The authors declare no competing financial interest.

ACKNOWLEDGMENTS

We thank Department of Biotechnology (DBT), India, for supporting this work with a rapid young investigators grant to R.B. (RGYI; BT/PR13125/GBD/27/193/2009). C.G.M. is grateful to Amrita Centre for Nanosciences and Molecular Medicine, Amrita Vishwa Vidyapeetham for computational infrastructure support funded by DBT-India under Nanotoxicology and Nanomedicine-Phase-II Program (Grant No. BT/PR14920/NNT/28/503/2010). A.C.P. is supported by Kerala State Council for Science, Technology & Environment (KSCSTE), with a junior research fellowship (Order No:1132/2013/KSCSTE), India. N.N. is supported by a senior research fellowship (Order No:45/16/2011/IMM-BMS) from ICMR, India.

ABBREVIATIONS

S. aureus, *Staphylococcus aureus*; *oatA*, *O*-acetyl transferase; PG, peptidoglycan; NAM, *N*-acetylmuramic acid; NAG, *N*-acetyl glucosamine; HEWL, hen egg white lysozyme; HL, human lysozyme; BE, binding energy; MD, molecular dynamics; W, water; SDS, sodium dodecyl sulfate; HFA, hydrofluoric acid; PDB, Protein Data Bank; GLIDE, grid-based ligand docking with energetics; SP, simple precision; XP, extra precision; SPC, simple point charge

REFERENCES

(1) Phillips, D. C. The Three-dimensional Structure of an Enzyme Molecule. *Sci. Am.* **1966**, *215*, 78−90.

(2) Phillips, D. C. The Hen Egg White Lysozyme Molecule. *Proc. Natl. Acad. Sci. U.S.A.* **1967**, *57*, 484−495.

(3) Düring, K.; Porsch, P.; Mahn, A.; Brinkmann, O.; Gieffers, W. The Non-enzymatic Microbicidal Activity of Lysozymes. *FEBS Lett.* **1999**, *449*, 93−100.

(4) Peschel, A.; Otto, M.; Jack, R. W.; Kalbacher, H.; Jung, G.; Götz, F. Inactivation of the dlt Operon in Staphylococcus aureus Confers Sensitivity to Defensins, Protegrins, and Other Antimicrobial Peptides. *J. Biol. Chem.* **1999**, *274*, 8405−8410.

(5) Herbert, S.; Bera, A.; Nerz, C.; Kraus, D.; Peschel, A.; Goerke, C.; Meehl, M.; Cheung, A.; Götz, F. Molecular Basis of Resistance to Muramidase and Cationic Antimicrobial Peptide Activity of Lysozyme in Staphylococci. *PLoS Pathog.* **2007**, *3*, e102.

(6) Bera, A.; Biswas, R.; Herbert, S.; Kulauzovic, E.; Weidenmaier, C.; Peschel, A.; Gotz, F. Influence of Wall Teichoic acid on Lysozyme Resistance in *Staphylococcus aureus*. *J. Bacteriol.* **2007**, *189*, 280−283.

(7) Imoto, T.; Johnson, L. N.; North, A. C. T.; Phillips, D. C.; Rupley, J. A. In *The Enzymes*, 3rd ed.; Boyer, P. D., Ed.; Academic Press: New York, 1972; pp 665−868.

(8) Ogata, M.; Umemoto, N.; Ohnuma, T.; Numata, T.; Suzuki, A.; Usui, T.; Fukamizo, T. A novel Transition-state analogue for Lysozyme, 4-O-beta-tri-N-acetylchitotriosyl Moranoline, provided Evidence Supporting the Covalent Glycosyl-Enzyme Intermediate. *J. Biol. Chem.* **2013**, *288*, 6072−6082.

(9) Kelly, J. A.; Sielecki, A. R.; Sykes, B. D.; James, M. N.; Phillips, D. C. X-ray crystallography of the Binding of the Bacterial Cell Wall Trisaccharide NAM-NAG-NAM to Lysozyme. *Nature* **1979**, *282*, 875−878.

(10) Bera, A.; Herbert, S.; Jakob, A.; Vollmer, W.; Gotz, F. Why are Pathogenic Staphylococci so Lysozyme Resistant? The Peptidoglycan *O*-acetyltransferase OatA is the Major Determinant for Lysozyme Resistance of *Staphylococcus aureus*. *Mol. Microbiol.* **2005**, *55*, 778−787.

(11) Sukhithasri, V.; Nisha, N.; Biswas, L.; Anil Kumar, V.; Biswas, R. Innate immune Recognition of Microbial Cell Wall Components and Microbial Strategies to Evade such Recognitions. *Microbiol. Res.* **2013**, *168*, 396−406.

(12) Meroueh, S. O.; Bencze, K. Z.; Hesek, D.; Lee, M.; Fisher, J. F.; Stemmler, T. L.; Mobashery, S. Three-dimensional structure of the Bacterial Cell Wall Peptidoglycan. *Proc. Natl. Acad. Sci. U.S.A.* **2006**, *103*, 4404−4409.

(13) Davis, K. M.; Weiser, J. N. Modifications to the Peptidoglycan backbone help Bacteria to Establish Infection. *Infect. Immun.* **2011**, *79*, 562−570.

(14) Bera, A.; Biswas, R.; Herbert, S.; Gotz, F. The presence of Peptidoglycan *O*-acetyltransferase in various Staphylococcal species Correlates with Lysozyme Resistance and Pathogenicity. *Infect. Immun.* **2006**, *74*, 4598−4604.

(15) Vollmer, W.; Blanot, D.; de Pedro, M. A. Peptidoglycan Structure and Architecture. *FEMS Microbiol. Rev.* **2008**, *32*, 149−167.

(16) Laurent, H.; Pascal, C.; Riccardo, T.; Maurizio, S.; Marie-Pierre, C.; Yanick, A.; Abdellah, B. *Enterococcus faecalis* Constitutes an Unusual Bacterial Model in Lysozyme Resistance. *Infect. Immun.* **2007**, *75*, 5390−5398.

(17) Guariglia-Oropeza, V.1.; Helmann, J. D. *Bacillus subtilis* σ(V) confers Lysozyme Resistance by Activation of Two Cell Wall Modification Pathways, Peptidoglycan O-acetylation and D-alanylation of Teichoic Acids. *J. Bacteriol.* **2011**, *193*, 6223−6232.

(18) Laaberki, M. H.; Pfeffer, J.; Clarke, A. J.; Dworkin, J. O-Acetylation of Peptidoglycan is required for proper Cell Separation and S-layer Anchoring in *Bacillus anthracis*. *J. Biol. Chem.* **2011**, *286*, 5278−5288.

(19) Veiga, P.; Bulbarela-Sampieri, C.; Furlan, S.; Maisons, A.; Chapot-Chartier, M. P.; Erkelenz, M.; Mervelet, P.; Noirot, P.; Frees, D.; Kuipers, O. P.; Kok, J.; Gruss, A.; Buist, G.; Kulakauskas, S. SpxB regulates O-acetylation-dependent Resistance of *Lactococcus lactis* Peptidoglycan to Hydrolysis. *J. Biol. Chem.* **2007**, *282*, 19342−19354.

(20) Davis, K. M.; Akinbi, H. T.; Standish, A. J.; Weiser, J. N. Resistance to Mucosal Lysozyme Compensates for the Fitness Deficit of Peptidoglycan Modifications by *Streptococcus pneumoniae*. *PLoS Pathog.* **2008**, *12*, No. e1000241.

(21) Iordanescu, S.; Surdeanu, M. Two Restriction and Modification systems in *Staphylococcus aureus* NCTC8325. *J. Gen. Microbiol.* **1976**, *96*, 277−281.

(22) Varma, P.; Nisha, N.; Dinesh, K. R.; Kumar, A. V.; Biswas, R. Anti-infective Properties of Lactobacillus fermentum against Staphylococcus aureus and Pseudomonas aeruginosa. *J. Mol. Microbiol. Biotechnol.* **2011**, *20*, 137−143.

(23) Biswas, R.; Martinez, R. E.; Gohring, N.; Schlag, M.; Josten, M.; Xia, G.; Hegler, F.; Gekeler, C.; Gleske, A. K.; Gotz, F.; Sahl, H. G.; Kappler, A.; Peschel, A. Proton-binding capacity of Staphylococcus aureus wall Teichoic acid and its role in Controlling Autolysin Activity. *PLoS One* **2012**, *7*, No. e41415.

(24) Fedtke, I.; Mader, D.; Kohler, T.; Moll, H.; Nicholson, G.; Biswas, R.; Henseler, K.; Gotz, F.; Zahringer, U.; Peschel, A. A Staphylococcus aureus ypfP Mutant with Strongly Reduced Lipoteichoic acid (LTA) content: LTA governs Bacterial Surface Properties and Autolysin Activity. *Mol. Microbiol.* **2007**, *65*, 1078−1091.

(25) Edwards, A. M.; Potts, J. R.; Josefsson, E.; Massey, R. C. Staphylococcus aureus host cell Invasion and Virulence in Sepsis is

DOI: 10.1021/ci500734k
J. Chem. Inf. Model. 2015, 55, 760−770

Facilitated by the Multiple Repeats within FnBPA. *PLoS Pathog.* **2010**, *6*, No. e1000964.
(26) Shoyama, Y.; Tamada, T.; Nitta, K.; Kumagai, I.; Kuroki, R.; Koshiba, T. Crystal structure of Human Lysozyme from Urine. 2009, DOI:10.2210/pdb2zil/pdb. Included in Bernstein, F. C.; Koetzle, T. F.; Williams, G. J.; Meyer, E. F., Jr.; Brice, M. D.; Rodgers, J. R.; Kennard, O.; Shimanouchi, T.; Tasumi, M. The Protein Data Bank: a Computer-based Archival file for Macromolecular Structures. *J. Mol. Biol.* **1977**, *112*, 535−542.
(27) Schrödinger, LLC, New York, NY, 2011.
(28) Friesner, R. A.; Murphy, R. B.; Repasky, M. P.; Frye, L. L.; Greenwood, J. R.; Halgren, T. A.; Sanschagrin, P. C.; Mainz, D. T. Extra precision Glide: Docking and Scoring Incorporating a model of Hydrophobic Enclosure for Protein-Ligand Complexes. *J. Med. Chem.* **2006**, *49*, 6177−6196.
(29) Torsteinsdottir, I.; Hakansson, L.; Hallgren, R.; Gudbjornsson, B.; Arvidson, N. G.; Venge, P. Serum Lysozyme: a Potential Marker of Monocyte/macrophage Activity in Rheumatoid Arthritis. *Rheumatology (Oxford)* **1999**, *38*, 1249−1254.
(30) Saari, K. M.; Aine, E.; Posz, A.; Klockars, M. Lysozyme Content of Tears in Normal Subjects and in Patients with External Eye Infections. *Graefe's Arch. Clin. Exp. Ophthalmol.* **1983**, *221*, 86−88.
(31) Perera, S.; Uddin, M.; Hayes, J. A. Salivary lysozyme: a Noninvasive Marker for the Study of the Effects of Stress of Natural Immunity. *Int. J. Behav. Med.* **1997**, *4*, 170−178.
(32) Bohnuud, T.; Kozakov, D.; Vajda, S. Evidence of Conformational Selection Driving the formation of Ligand Binding Sites in Protein-Protein Interfaces. *PLoS Comput. Biol.* **2014**, *10*, No. e1003872.
(33) Kumar, V.; Saravanan, P.; Arvind, A.; Mohan, C. G. Identification of Hotspot Regions of MurB Oxidoreductase Enzyme using Homology Modeling, Molecular Dynamics and Molecular Docking Techniques. *J. Mol. Model.* **2011**, *17*, 939−953.
(34) Gupta, S.; Fallarero, A.; Jarvinen, P.; Karlsson, D.; Johnson, M. S.; Vuorela, P. M.; Mohan, C. G. Discovery of Dual Binding Site Acetylcholinesterase Inhibitors identified by Pharmacophore Modeling and Sequential Virtual Screening Techniques. *Bioorg. Med. Chem. Lett.* **2011**, *21*, 1105−1112.
(35) Victor, M. R.; Marc, D.; Tillmann, H.; Agustí, L.; Tilman, S.; Thomas, R. W.; Jean-Didier, M. Structural-, Kinetic- and Docking Studies of Artificial Imine Reductases based on the Biotin-Streptavidin Technology: An Induced Lock-and-Key Hypothesis. *J. Am. Chem. Soc.* **2014**, *136*, 15676−15683.
(36) Agostino, M.; Jene, C.; Boyle, T.; Ramsland, P. A.; Yuriev, E. Molecular Docking of Carbohydrate Ligands to Antibodies: Structural Validation against Crystal Structures. *J. Chem. Inf. Model.* **2009**, *49*, 2749−2760.
(37) Koshland, D. E. Stereochemistry and Mechanism of Enzymatic Reactions. *Biol. Rev. Cambridge Philos. Soc.* **1953**, *28*, 416−436.
(38) Vocadlo, D. J.; Davies, G. J.; Laine, R.; Withers, S. G. Catalysis by Hen Egg-white Lysozyme Proceeds via a Covalent Intermediate. *Nature* **2001**, *412*, 835−838 and references cited therein.
(39) (a) Karplus, M.; Petsko, G. A. Molecular Dynamics Simulations in Biology. *Nature* **1990**, *347*, 631−639. (b) Calimet, N.; Simoes, M.; Changeux, J. P.; Karplus, M.; Taly, A.; Cecchini, M. A Gating Mechanism of Pentameric Ligand-gated Ion Channels. *Proc. Natl. Acad. Sci. U.S.A.* **2013**, *110*, E3987−E3996.
(40) Jain, V.; Saravanan, P.; Arvind, A.; Mohan, C. G. First Pharmacophore model of CCR3 receptor Antagonists and its Homology Model-assisted, Stepwise Virtual Screening. *Chem. Biol. Drug Des.* **2011**, *77*, 373−387.
(41) Ashish, P.; Jigneshkumar, P.; Sathyaprakash, T.; Mohan, C. G. Harnessing Human N-type Ca^{2+} Channel Receptor by Identifying the Atomic Hot-Spot Regions for its Structure-Based Blocker Design. *Mol. Inf.* **2012**, *31*, 643−657.
(42) Campbell, A. J.; Lamb, M. L.; Joseph-McCarthy, D. Ensemble-Based Docking using Biased Molecular Dynamics. *J. Chem. Inf. Model.* **2014**, *54*, 2127−2138.
(43) Clarke, A. J.; Dupont, C. O-acetylated Peptidoglycan: its Occurrence, Pathobiological Significance, and Biosynthesis. *Can. J. Microbiol.* **1992**, *38*, 85−91.
(44) Post, C. B.; Brooks, B. R.; Karplus, M.; Dobson, C. M.; Artymiuk, P. J.; Cheetham, J. C.; Phillips, D. C. Molecular Dynamics Simulations of Native and Substrate-bound Lysozyme. A study of the Average Structures and Atomic Fluctuations. *J. Mol. Biol.* **1986**, *190*, 455−479.

DOI: 10.1021/ci500734k
J. Chem. Inf. Model. 2015, 55, 760−770